

Melting, freezing, sublimation, and phase coexistence in sodium chloride nanocrystals

Gary A. Breaux, Robert C. Benirschke, and Martin F. Jarrold^{a)}
Chemistry Department, Indiana University, Bloomington, Indiana 47405-7102

(Received 17 June 2004; accepted 7 July 2004)

Calorimetry measurements, performed by multicollision induced dissociation, have been used to probe the melting of a number of $(\text{NaCl})_n\text{Na}^+$ clusters with $n=22-37$. The clusters anneal at 225–325 K and melt at 750–850 K. $(\text{NaCl})_{22}\text{Na}^+$ and $(\text{NaCl})_{37}\text{Na}^+$, which can adopt geometries that are perfect fragments of the bulk lattice melt at around 850 K. The other clusters, which (except for $n=31$) must have defects, melt at temperatures which are up to 100 K lower than the perfect nanocrystals. The internal energy distributions become bimodal near the melting temperature. This is the signature of slow dynamic phase coexistence where clusters spontaneously jump back and forth between the solid and liquid states with an average period that is longer than required for thermal equilibration. The jump frequency must be between 10^4 and 10^7 s^{-1} for the bimodal distribution to be observable in our experiments. The $(\text{NaCl})_n\text{Na}^+$ clusters can dissociate by an unusual thermally activated process where melting and freezing raise the internal energy to generate hot solid clusters that can sublime before they cool to the ambient temperature. © 2004 American Institute of Physics. [DOI: 10.1063/1.1786921]

I. INTRODUCTION

In the mesoscopic size regime (particles with thousands of atoms) melting points are depressed relative to the bulk value because of the increase in the surface to volume ratio.^{1–3} In the cluster size regime (<500 atoms) the simple thermodynamic scaling responsible for the melting point depression breaks down and clusters have melting temperatures that fluctuate with the number of atoms,^{4–6} in some cases by hundreds of degrees.⁷ These fluctuations are not strongly correlated with geometric or electronic shells closings and their origin remains poorly understood.

Melting in the cluster size regime differs from the melting of a macroscopic object in a number of ways. The melting transition for a cluster is broadened (there is no longer a melting point) and the liquid and solid phases coexist over a range of temperatures. In the coexistence region, simulations suggest that clusters can repetitively switch back and forth between being entirely solid and entirely liquid.^{8–13} There is no analog for this behavior with bulk materials. When a macroscopic object melts, the liquid and solid phases coexist in contact. It is possible to distinguish between the dynamic phase coexistence of a cluster and the static phase coexistence of a macroscopic object from their internal energy distributions. For a macroscopic object the internal energy distribution at the melting point has a single narrow component, and the average internal energy changes smoothly from that of the solid to that of the liquid. The same is true for an ensemble of clusters, if they rapidly switch back and forth between the liquid and solid states so that their internal energies are not equilibrated in either phase. However, if transitions between the solid and liquid phases occur sufficiently infrequently that the clusters can become equilibrated as solid and liquid, the internal energy distribution of the en-

semble is bimodal (with one component for each phase). Haberland and collaborators recently reported indirect evidence that Na_{147}^+ has a bimodal energy distribution at its melting transition.¹⁴ The bimodal energy distribution occurs for finite systems because there is a free energy barrier between the solid and liquid states. The barrier results from the energetic cost of the interface associated with phase separation.¹⁵

Alkali halide clusters adopt bulklike structures at small sizes,^{16–20} and hence they are interesting model systems to examine melting in the cluster size regime. They can be modeled using simple potentials and several groups have performed simulations of their melting transitions.^{11,21,22} Alkali halide clusters show magic numbers due to cubic packing. $(\text{NaCl})_{37}\text{Na}^+$, for example, adopts a $3 \times 5 \times 5$ cuboid structure (the $j \times k \times l$ labels give the number of atoms along each edge). This structure is a true nanocrystal. $(\text{NaCl})_{36}\text{Na}^+$, with one fewer NaCl unit, must possess at least one defect. We have examined the melting of the $3 \times 3 \times 5$ and $3 \times 5 \times 5$ nanocrystals, $(\text{NaCl})_{22}\text{Na}^+$ and $(\text{NaCl})_{37}\text{Na}^+$, as well as a number of clusters with n between 22 and 37 that have defects. We find that clusters with defects melt at temperatures that are up to 100 K lower than the perfect nanocrystals.

The melting transitions are probed using a new approach to doing calorimetry on unsupported clusters based on multicollision-induced dissociation.²³ The amount of energy required to dissociate an ensemble of size-selected clusters decreases as the temperature increases due to the clusters' thermal energy. At the melting transition, the latent heat causes a sharp drop in the energy required to cause dissociation, and this provides a thermodynamic signature of melting. For this approach to work properly, dissociation must occur from the liquid state. In our previous studies of gallium clusters this criteria was satisfied (the liquid clusters remain

^{a)}Electronic mail: mfj@indiana.edu

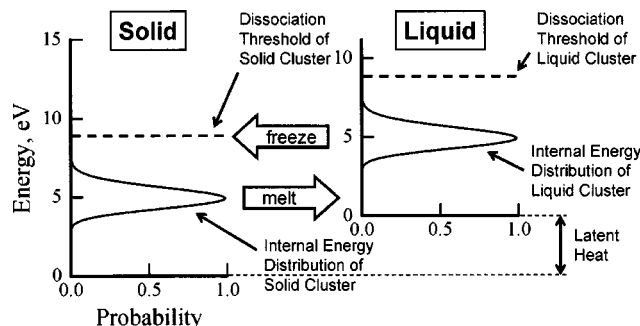


FIG. 1. Schematic diagram showing the relationship between the internal energy distributions and the dissociation thresholds of solid and liquid clusters. The plot is based on $(\text{NaCl})_{35}\text{Na}^+$.

intact to temperatures substantially above the melting transition).²¹ However, the $(\text{NaCl})_n\text{Na}^+$ clusters studied here sublime (see below). If the $(\text{NaCl})_n\text{Na}^+$ clusters were to simply remain solid and sublime when heated we would obviously not be able to measure a melting temperature. But our results indicate the $(\text{NaCl})_n\text{Na}^+$ clusters can melt and freeze before subliming. In fact, we will show that these melt-freeze cycles can drive the sublimation.

To better illustrate the relationship between melting, freezing, and sublimation, Fig. 1 shows a schematic diagram of the internal energy distributions and dissociation thresholds for solid and liquid $(\text{NaCl})_{35}\text{Na}^+$ clusters. We take the latent heat from the Monte Carlo simulations of Doye and Wales²⁰ for $(\text{NaCl})_{35}\text{Cl}^-$. The internal energy distributions were calculated at 800 K (which is the melting temperature according to our results presented below) using a Debye-like vibrational frequency distribution.²⁴ We assume that the density of states for the liquid clusters is increased by a factor of $\Delta\Omega = \exp(\Delta H_m/RT_m)$, where T_m is the melting temperature and ΔH_m is the latent heat ($\Delta S_m = \Delta H_m/T_m = R/n\Delta\Omega$). The dissociation thresholds shown in Fig. 1 represent the amount of energy required to cause fragmentation on the microsecond time scale of the multicollision-induced dissociation method employed here.²⁵ The threshold is not sharp as suggested by the line in the figure, the probability for dissociation increases smoothly from zero to one over a range of internal energies. The dissociation thresholds for the liquid and solid clusters are expected to be similar²⁶ (the vapor pressure of the bulk material does not show a discontinuity at the melting point²⁷). The dissociation threshold for the solid cluster shown in Fig. 1 was estimated from our experimental results, we assume the threshold for the liquid cluster is the same.

It is evident from Fig. 1 that the freezing of liquid clusters will initially generate hot solid clusters and the melting of solid clusters will initially generate cold liquid ones. The internal energies of the nascent melted or frozen cluster must be equilibrated after a transition. If the time scale for equilibration is less than the average interval between melting and freezing events then the solid and liquid clusters will have separate internal energy distributions, identical to those calculated from statistical thermodynamics (as in Fig. 1). If, on the other hand, the time scale for equilibration is greater than the average time spent in each of the phases, then equilibra-

tion cannot occur for the separate phases, and both phases will share a common internal energy distribution. In Fig. 1, the internal energies of the nascent frozen clusters are close to the dissociation threshold for the solid clusters. Thus the nascent frozen clusters will require much less energy to dissociate than the equilibrated solid and liquid clusters (the nascent frozen clusters may even spontaneously sublime). The sudden emergence of a component that requires much less additional energy to dissociate is the signature for these nascent frozen clusters. We have observed this behavior for the sodium chloride clusters studied here. We will show below that for the nascent frozen clusters to be observable in this way, the jumps between the liquid and solid phases must occur with a frequency between 10^4 and 10^7 s^{-1} .

II. EXPERIMENTAL METHODS

The main features of the experimental apparatus used for these studies have been described in detail previously.²¹ The sodium chloride clusters were produced in a gas aggregation source and ionized using a discharge located up-stream from the oven region. The temperature of the clusters is set before they exit the source in an 8.9 cm long temperature-variable (80–1000 K) extension. The cluster ions spend at least a millisecond in the extension where the helium buffer gas pressure is ≈ 10 Torr. Under the conditions employed, thermal equilibration is expected to occur on a 10^{-7} – 10^{-5} s time scale.²³ In our recent studies of gallium clusters, we performed a series of tests to confirm that the clusters had achieved thermal equilibrium with the walls of the extension.²¹ We adjusted the size of entrance and exit apertures so that the pressure in the extension varied by more than an order of magnitude. There was no effect on the measured thresholds. In the present work, we employed a conservative configuration with no restriction at the entrance to the extension. After exiting the extension, a specific cluster size is selected with a quadrupole mass spectrometer, and the size-selected clusters are focused into a high pressure collision cell which contains 1.00 Torr of helium. As the ions enter the collision cell, they are rapidly heated by many collisions with the helium gas. If the initial translational energy is high enough, the cluster ions dissociate. Some fraction of the parent and product ions are extracted from the collision cell and focused into a second quadrupole mass spectrometer where they are analyzed, and then detected.

III. RESULTS AND DISCUSSION

Product ion mass spectra resulting from multicollision-induced dissociation of $(\text{NaCl})_{27}\text{Na}^+$ and $(\text{NaCl})_{35}\text{Na}^+$ are shown in Fig. 2. The main dissociation pathways for $(\text{NaCl})_{27}\text{Na}^+$ are formation of $(\text{NaCl})_{22}\text{Na}^+$ and loss of $(\text{NaCl})_2$. The latter is an important dissociation pathway for all the clusters studied, while formation of $(\text{NaCl})_{22}\text{Na}^+$ is important for clusters with $n < 31$. $(\text{NaCl})_{22}\text{Na}^+$ ($3 \times 3 \times 5$) is a strong magic number in the cluster distribution from the source. For clusters with $n > 31$, $(\text{NaCl})_{31}\text{Na}^+$ is an important product ion. $(\text{NaCl})_{31}\text{Na}^+$ ($3 \times 3 \times 7$) is a weak magic number in the cluster distribution from the source. The preferential loss of $(\text{NaCl})_2$ rather than individual NaCl units

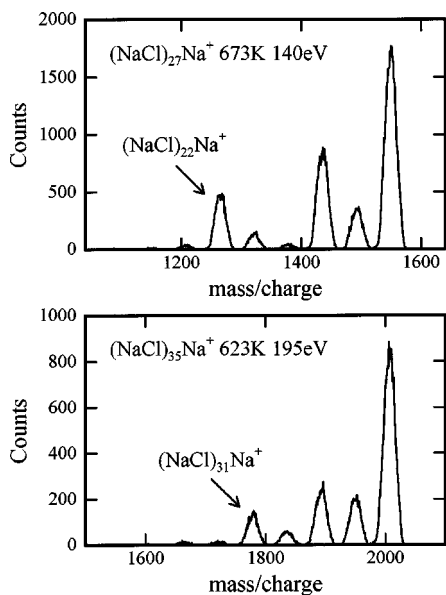


FIG. 2. Mass spectra recorded for multicollision-induced dissociation of $(\text{NaCl})_{27}\text{Na}^+$ and $(\text{NaCl})_{35}\text{Na}^+$. The conditions employed are shown on the plots.

(which is observed for almost all clusters) probably reflects the stability of the $(\text{NaCl})_2$ fragment [dissociation to $(\text{NaCl})_{n-2}\text{Na}^+ + (\text{NaCl})_2$ is lower in energy than $(\text{NaCl})_{n-1}\text{Na}^+ + \text{NaCl}$]. The preference for magic number fragments such as $(\text{NaCl})_{22}\text{Na}^+$ and $(\text{NaCl})_{31}\text{Na}^+$ is significant because this observation is not consistent with dissociation from the liquid state. This was noted in previous studies of the fragmentation of sodium fluoride clusters, where it was taken to indicate that the clusters must dissociate from the solid state.¹⁷

Multicollision-induced dissociation can be used to perform calorimetry measurements by tracking the median internal energy of the clusters as a function of their temperature. To accomplish this, the fraction of the parent cluster ions that dissociate is determined from product ion mass spectra. This quantity is then monitored as a function of the ions' translational energy (TE). Measurements performed at different TEs show a threshold behavior, and the TE required for 50% of the ions to dissociate (TE50%D) is obtained from the results using a linear regression. The TE50%D values are then determined as a function of the temperature of the source extension.

Figure 3(a) shows a plot of TE50%D against temperature for $(\text{NaCl})_{35}\text{Na}^+$. The TE50%D values decrease as the temperature is raised because of the increase in the cluster's internal energy. The derivative of TE50%D with temperature ($-\partial\text{TE50\%D}/\partial T$) is approximately proportional to the cluster's heat capacity. The proportionality constant is the fraction of the ion's translational energy that is converted into internal energy as the ions enter the collision cell. This can be estimated using a simple impulsive collision model.²⁸ For the $(\text{NaCl})_n\text{Na}^+$ clusters studied here, the fraction is estimated to be ≈ 0.05 . Because this fraction is so small, changes in the internal energy of the cluster are amplified and lead to large changes in the TE required for dissociation. The histogram in Fig. 1(a) shows the heat capacities derived from the

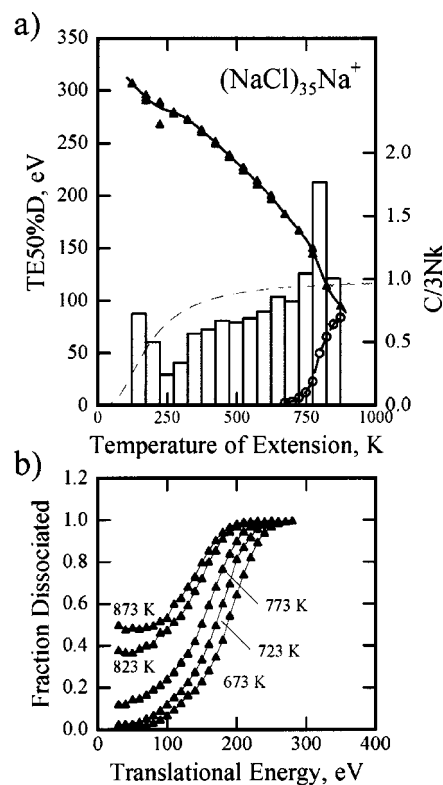


FIG. 3. (a) Shows a plot of TE50%D against temperature of the source extension for $(\text{NaCl})_{35}\text{Na}^+$. The points are the measured values and the line through the points is a spline fit. The histogram shows the cluster's heat capacity derived from the TE50%D values (see text). The heat capacities scale on the right-hand side of the plot is $C/3Nk$, where $3N = 3(2n + 1) - 4.5$ (n is the number of NaCl units). The thin-dashed line shows the heat capacity calculated using a modified Debye model (see text). The unfilled circles and thick-dashed line shows the fraction dissociated at a TE of 50 eV. (b) Shows the fraction dissociated as a function of the TE for source extension temperatures ≈ 800 K.

TE50%D values and the thin-dashed line shows the heat capacities calculated using statistical mechanics (the rotational contribution is assumed to be classical and the vibrational component is determined from a modified Debye model that incorporates a low frequency cutoff to account for the finite size of the cluster²⁹).

There is an inflection (or jump) in the TE50%D values at ≈ 225 – 325 K in Fig. 3(a), and a corresponding minimum in the heat capacity. This is attributed to the presence of high energy isomers. As the temperature is raised, the isomers anneal into lower energy structures, and larger TEs are then needed to cause dissociation. The average change in the potential energy that occurs when the isomers anneal can be estimated from the jump in the TE50%D values using the fraction of the TE that is converted into internal energy (≈ 0.05 from above). For $(\text{NaCl})_{35}\text{Na}^+$ the potential energy decrease on annealing was estimated to be ≈ 1.0 eV. Structural transitions have previously been observed for $(\text{NaCl})_{35}\text{Cl}^-$ at ≈ 273 – 323 K using high-resolution ion mobility measurements.³⁰ However, these were assigned to transitions between low energy isomers (< 0.2 eV above the ground state) on the basis of calculations.²⁰ The higher energy isomers responsible for the changes observed here are probably partially amorphous structures that are generated by

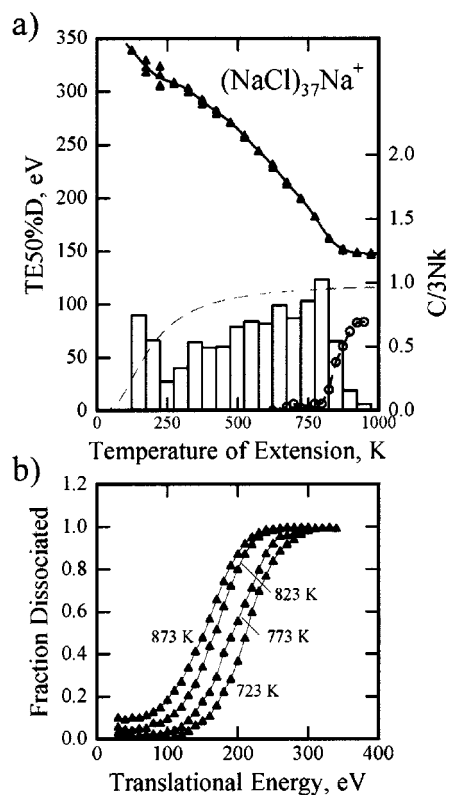


FIG. 4. Same as Fig. 3 but for $(\text{NaCl})_{37}\text{Na}^+$.

further cluster growth in the extension when it is cooled. Low temperature inflections in the TE50%D values were also found for $(\text{NaCl})_n\text{Na}^+$ with $n=27, 36,$ and 37 . The estimated potential energy changes for these annealing processes were comparable (0.66, 0.89, and 0.78 eV, respectively).

There is a sharp decrease in the TE50%D values for $(\text{NaCl})_{35}\text{Na}^+$ at ≈ 800 K and a corresponding spike in the heat capacity (see Fig. 3). The inflection and spike are smaller than expected for the latent heat of fusion [assuming the latent heat of $(\text{NaCl})_{35}\text{Na}^+$ is the same as the value for $(\text{NaCl})_{35}\text{Cl}^-$ obtained from Monte Carlo simulations²⁰]. However, the presence of magic fragments suggests that these clusters dissociate from the solid state, in which case an inflection and spike are not expected at all. We will show below that the inflection observed at ≈ 800 K probably results from changes in the internal energy distributions due to melting and freezing transitions that occur prior to dissociation from the solid state. Figure 3(b) shows the fraction of $(\text{NaCl})_{35}\text{Na}^+$ that dissociates plotted against the TE for several extension temperatures ≈ 800 K (the spike in the heat capacity). For temperatures above 723 K a tail develops at low TEs. This tail indicates that some of the clusters have substantially increased internal energies. The only plausible explanation for the sudden appearance of these “hot” clusters is that they result from liquid clusters that have frozen either in the source extension or on the way from the extension to the collision cell. If freezing occurred in the source extension, it must have occurred sufficiently close to the exit that the internal energy distribution of the nascent solid clusters is not fully equilibrated. Thermalization is expected to

occur on a $0.1\text{--}10\ \mu\text{s}$ time scale in the extension,²³ while the flight time from the source extension to the collision cell is $\approx 100\ \mu\text{s}$. Thus the frequency of the jumps between the phases must be $>10^4\ \text{s}^{-1}$. The hot solid clusters generated by the freezing of liquid clusters may spontaneously sublime as they travel from the heated extension to the collision cell. If fragmentation occurs before or in the quadrupole mass spectrometer, the majority of the products will be lost. However, products that form after the quadrupole (or very near the end of the quadrupole) will contribute to the low energy tails in Fig. 3(b).

The presence of the tail in Fig. 3(b) and the threshold at higher energies, which is due to the dissociation of equilibrated solid clusters (and perhaps unfrozen liquid clusters), indicates that there is a bimodal energy distribution for $(\text{NaCl})_{35}\text{Na}^+$ at its melting transition. For a bimodal energy distribution to be established the average period between the melting and freezing transitions must be greater than the time scale for equilibration of the phases. Equilibration is expected to occur on a $0.1\text{--}10\ \mu\text{s}$ time scale in the extension,²³ so the frequency of transitions between the phases must be $<10^7\ \text{s}^{-1}$. Combining this with the limit from above, we can bracket the transition frequency as being between 10^4 and $10^7\ \text{s}^{-1}$. A slow dynamic phase coexistence has been observed in molecular dynamics simulations for $(\text{KCl})_{32}$ where it appears that the transition frequency is around $10^8\ \text{s}^{-1}$.^{11,12}

Near the melting transition, the clusters must undergo a series of melting and freezing cycles as they travel through the heated extension, and each freezing transition should generate hot solid clusters of which some fraction may spontaneously dissociate before their internal energy is thermalized. Thus a sharp decrease in the $(\text{NaCl})_{35}\text{Na}^+$ parent ion intensity is predicted. Such a decrease is observed, the $(\text{NaCl})_{35}\text{Na}^+$ signal starts to decline ≈ 800 K, and almost completely disappears above 900 K.

Figure 4(a) shows a plot of TE50%D against temperature for $(\text{NaCl})_{37}\text{Na}^+$. At temperatures above 800 K the TE50%D values level off instead of decreasing as observed for $(\text{NaCl})_{35}\text{Na}^+$. At the same time the $(\text{NaCl})_{37}\text{Na}^+$ signal intensity decreases sharply. In the plots of the fraction dissociated against TE, Fig. 4(b), a tail grows in at low TEs for temperatures above 800 K, but it is significantly smaller than for $(\text{NaCl})_{35}\text{Na}^+$. All these observations are consistent with the idea that a larger fraction of the hot solid clusters (generated by freezing liquid clusters) spontaneously fragment for $(\text{NaCl})_{37}\text{Na}^+$ than for $(\text{NaCl})_{35}\text{Na}^+$. This may be due to $(\text{NaCl})_{37}\text{Na}^+$ having a larger heat of fusion and a higher melting temperature than $(\text{NaCl})_{35}\text{Na}^+$. The TE50%D values for $(\text{NaCl})_{37}\text{Na}^+$ level off because most of the liquid clusters do not survive, so the TE50%D values reflect the average internal energy of the remaining solid clusters.

The fraction of $(\text{NaCl})_{35}\text{Na}^+$ and $(\text{NaCl})_{37}\text{Na}^+$ dissociated at a TE of 50 eV provides a metric for the fraction of liquid clusters present. This quantity shows a threshold behavior when plotted against temperature (circles and thick dashed lines in Figs. 3 and 4). We expect these thresholds to be correlated with the melting temperatures. From the spike in the heat capacity we assign a melting temperature of ≈ 800 K to $(\text{NaCl})_{35}\text{Na}^+$ and from the fraction dissociated at

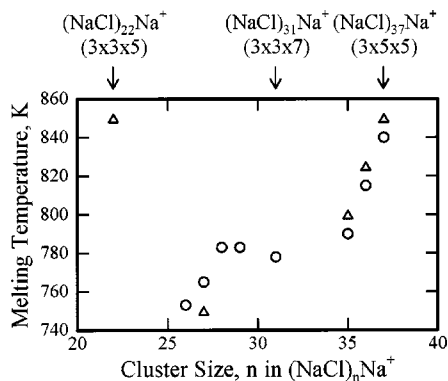


FIG. 5. Plot of the melting temperatures determined for $(\text{NaCl})_n\text{Na}^+$ clusters with $n=22$ –37. The triangles show values determined from the heat capacity plots and the circles show values obtained from the fraction dissociated at a TE of 50 eV (see text). The estimated uncertainty is ± 25 K.

a TE of 50 eV we determine a melting temperature of ≈ 790 K. For $(\text{NaCl})_{37}\text{Na}^+$ we estimate a melting temperature of 850 K from the heat capacity plot and from the fraction dissociated at a TE of 50 eV we obtain a value of 840 K. Thus the melting temperature of $(\text{NaCl})_{37}\text{Na}^+$ is ≈ 50 K higher than for $(\text{NaCl})_{35}\text{Na}^+$. Measurements were also performed for $(\text{NaCl})_n\text{Na}^+$ clusters with $n=22$, 27, and 36 (22 is a magic number, 27 and 36 are not). The TE50%D plots for $(\text{NaCl})_{27}\text{Na}^+$ and $(\text{NaCl})_{36}\text{Na}^+$ show a maximum in the heat capacity like that for $(\text{NaCl})_{35}\text{Na}^+$. The TE50%D plot for $(\text{NaCl})_{22}\text{Na}^+$ is similar to that for $(\text{NaCl})_{37}\text{Na}^+$ (i.e., the TE50%D values level off).

Measuring the fraction dissociated at a TE of 50 eV provides a more convenient way to determine the melting temperatures than measuring the full TE50%D plots. These measurements were performed for a number of $(\text{NaCl})_n\text{Na}^+$ clusters with n between 22 and 37. Figure 5 shows the melting temperatures determined by both methods plotted against cluster size. The estimated uncertainty is ± 25 K. The two magic number cuboid clusters have the highest melting temperatures (≈ 850 K). The melting point of bulk sodium chloride is 1074 K, so the clusters have depressed melting temperatures. While depressed melting points are expected in the mesoscopic size regime (thousands of atoms) in the cluster size regime, some metals (tin and gallium) have elevated melting points^{7,21,31} which probably result from the clusters having different structures than the bulk. Thus the $(\text{NaCl})_n\text{Na}^+$ clusters have depressed melting points because they have bulklike geometries. According to the Monte Carlo simulations of Doye and Wales,²⁰ $(\text{NaCl})_{35}\text{Cl}^-$ melts at ≈ 700 K, which is in reasonable agreement with our value of 800 K for $(\text{NaCl})_{35}\text{Na}^+$. The magic number clusters have the highest melting temperatures (≈ 850 K). The other clusters [except $(\text{NaCl})_{31}\text{Na}^+$] have geometries which must possess defects. $(\text{NaCl})_{31}\text{Na}^+$ may have a $3 \times 3 \times 7$ geometry; though it appears as a magic number in the fragmentation of clusters with $n > 31$, $(\text{NaCl})_{31}\text{Na}^+$ is a weak magic number in the distribution of clusters from the source. The $3 \times 3 \times 7$ geometry is evidently “less magic” than the $3 \times 3 \times 5$ and the $3 \times 5 \times 5$ geometries, presumably because its elongated shape leads to a higher surface energy. The melting temperature of

$(\text{NaCl})_{31}\text{Na}^+$ is not elevated like that of $(\text{NaCl})_{22}\text{Na}^+$ and $(\text{NaCl})_{37}\text{Na}^+$.

IV. CONCLUSIONS

We have used multicollision-induced dissociation based calorimetry to probe the melting of some $(\text{NaCl})_n\text{Na}^+$ clusters with $n=22$ –37. The clusters melt at 750–850 K, which is well below the bulk melting point of 1074 K. Annealing transitions (probably from high energy amorphous structures) were observed at 225–325 K. Thus there is a clear separation between isomerization and melting. This distinction is often not clear for smaller clusters. The melting temperatures are correlated with the geometric structure, the $(\text{NaCl})_{22}\text{Na}^+$ and $(\text{NaCl})_{37}\text{Na}^+$ clusters with perfect nanocrystal geometries have the highest melting temperatures. The presence of a defect lowers the melting temperature by up to 100 K. The internal energy distributions become bimodal near the melting temperature. This is the signature of slow dynamic phase coexistence where clusters spontaneously jump back and forth between being entirely solid and entirely liquid on a time scale that is longer than required for thermal equilibration. The jump frequency must be between 10^4 and 10^7 s⁻¹ for the bimodal distribution to be observable in our experiments. $(\text{NaCl})_n\text{Na}^+$ clusters can dissociate via an unusual thermally activated process where a melting and freezing cycle pumps up the internal energy to generate hot solid clusters that sublime before cooling to the ambient temperature.

ACKNOWLEDGMENT

We gratefully acknowledge the support of the National Science Foundation.

- P. Pawlow, Z. Phys. Chem. **65**, 1 (1909).
- M. J. Takagi, J. Phys. Soc. Jpn. **9**, 359 (1954).
- Ph. Buffat and J. P. Borel, Phys. Rev. A **13**, 2287 (1976).
- M. Schmidt, R. Kusche, W. Kronmüller, B. von Issendorff, and H. Haberland, Phys. Rev. Lett. **79**, 99 (1997).
- M. Schmidt, R. Kusche, B. von Issendorff, and H. Haberland, Nature (London) **393**, 238 (1998).
- M. Schmidt and H. Haberland, C. R. Phys. **3**, 327 (2002).
- G. A. Breaux, D. A. Hillman, C. M. Neal, R. C. Benirschke, and M. F. Jarrold, J. Am. Chem. Soc. **126**, 8628 (2004).
- R. D. Etters and J. B. Kaelberer, J. Chem. Phys. **66**, 5112 (1977).
- J. Jellinek, T. L. Beck, and R. S. Berry, J. Chem. Phys. **84**, 2783 (1986).
- J. P. Rose and R. S. Berry, J. Chem. Phys. **96**, 517 (1992).
- J. P. Rose and R. S. Berry, J. Chem. Phys. **98**, 3246 (1993).
- D. J. Wales and R. S. Berry, Phys. Rev. Lett. **73**, 2875 (1994).
- B. Vekhter and R. S. Berry, J. Chem. Phys. **106**, 6456 (1997).
- M. Schmidt, R. Kusche, T. Hippler, J. Donges, W. Kronmüller, B. von Issendorff, and H. Haberland, Phys. Rev. Lett. **86**, 1191 (2001).
- D. J. Wales and J. P. K. Doye, J. Chem. Phys. **103**, 3061 (1995).
- J. E. Campana, T. M. Barlak, R. J. Colton, J. J. DeCorpo, J. R. Wyatt, and B. I. Dunlap, Phys. Rev. Lett. **47**, 1046 (1981).
- R. Pflaum, K. Sattler, and E. Recknagel, Chem. Phys. Lett. **138**, 8 (1987).
- Y. J. Twu, C. W. S. Conover, Y. A. Yang, and L. A. Bloomfield, Phys. Rev. B **42**, 5306 (1990).
- R. D. Beck, P. St. John, M. L. Homer, and R. L. Whetten, Science **253**, 879 (1991).
- Ph. Dugourd, R. R. Hudgins, and M. F. Jarrold, Chem. Phys. Lett. **267**, 186 (1997).
- J. Luo, U. Landman, and J. Jortner, in *Physics and Chemistry of Small*

- Clusters*, edited by P. Jena, B. K. Rao, and S. N. K. Khanna, NATO ASI Series B Physics, Vol. 158 (Plenum, New York, 1987), p. 201.
- ²²J. P. K. Doye and D. J. Wales, *J. Chem. Phys.* **111**, 11070 (1999).
- ²³G. A. Breaux, R. C. Benirschke, T. Sugai, B. S. Kinnear, and M. F. Jarrold, *Phys. Rev. Lett.* **91**, 215508 (2003).
- ²⁴U. Ray, M. F. Jarrold, J. E. Bower, and J. S. Krauss, *J. Chem. Phys.* **91**, 2912 (1989).
- ²⁵M. F. Jarrold and E. C. Honea, *J. Am. Chem. Soc.* **114**, 459 (1992).
- ²⁶A simple thermodynamic cycle indicates that the dissociation energy of the liquid cluster should be larger than that of the solid by the difference between the latent heats of the intact cluster and its products.
- ²⁷C. T. Ewing and K. H. Stern, *J. Phys. Chem.* **78**, 1998 (1974).
- ²⁸M. F. Jarrold and E. C. Honea, *J. Phys. Chem.* **95**, 9181 (1991).
- ²⁹J. Bohr, *Int. J. Quantum Chem.* **84**, 249 (2001).
- ³⁰R. R. Hudgins, Ph. Dugourd, J. M. Tenenbaum, and M. F. Jarrold, *Phys. Rev. Lett.* **78**, 4213 (1997).
- ³¹A. A. Shvartsburg and M. F. Jarrold, *Phys. Rev. Lett.* **85**, 2530 (2000).